DOI:
10.1016/j.ssnmr.2015.09.009

Document Version
Peer reviewed version

^{14}N NQR, relaxation and molecular dynamics of the explosive TNT☆

John A. S. Smith[a] , Michael D. Rowe*[a] , Kaspar Althoefer[a], Neil F. Peirson[b] and Jamie Barras[a].

[a]*Department of Informatics, King's College London, Strand, London, WC2R 2LS, U.K.*
[b]*Angel House, Marsh Lane, Saundby, Retford, DN22 9ES, U.K.*

☆This work was funded in part by the UK Defence Science and Technology Laboratory (DSTL).

*Corresponding author. Phone: +44 20 8994 0078

E-mail addresses: michael.d.rowe@kcl.ac.uk (Michael D. Rowe), k.althoefer@kcl.ac.uk (Kaspar Althoefer), nqr2004@yahoo.co.uk (Neil F. Peirson), jamie.barras@kcl.ac.uk (Jamie Barras).

Abstract

Multiple pulse sequences are widely used for signal enhancement in NQR detection applications. Since the various ^{14}N NQR relaxation times, signal decay times and frequency of each NQR line have a major influence on detection sequence performance, it is important to characterise these parameters and their temperature variation, as fully as possible. In this paper we discuss such measurements for a number of the ν_+ and ν_- NQR lines of monoclinic and orthorhombic TNT and relate the temperature variation results to molecular dynamics. The temperature variation of the ^{14}N spin-lattice relaxation times T_1 is interpreted as due to hindered rotation of the NO_2 group about the C–NO_2 bond with an activation energy of 89 kJ mol^{-1} for the ortho and para groups of monoclinic TNT and 70 kJ mol^{-1} for the para group of orthorhombic TNT.

Keywords: TNT detection, ^{14}N NQR, NQR relaxation times, NQR parameters, temperature variation, pulsed spin-locking (PSL) sequence.

1. Introduction

Many nitrogen compounds, particularly those containing nitro groups, such as the explosive 2,4,6-trinitrotoluene (TNT) $C_6H_2(NO_2)_3CH_3$ (Fig. 1) have ^{14}N nuclear quadrupole resonance (NQR) frequencies [1,2] below 1 MHz, where inductive methods of signal detection have poor sensitivity. In detection applications of NQR [3] various multiple pulse sequences are often used to improve sensitivity by rapidly regenerating signals. Optimisation of sensitivity is crucial and it is important to have full characterisation, including temperature variation, of the

various NQR parameters because of their influence on detection sequence performance. The main parameters are NQR line frequency, T_1 −the spin-lattice relaxation time, T_2 −the spin-spin relaxation time, T_2^* −the signal decay time and T_{2e} −the decay time of echo trains generated by multiple pulse sequences of the pulsed spin-locking (PSL) type [2 − 5]. This paper presents the results of such measurements for ν_+ and ν_- ^{14}N NQR lines of monoclinic and orthorhombic TNT. The temperature variation of the NQR frequencies and their assignment to specific nitrogen sites are discussed and the temperature dependence of relaxation times related to the molecular dynamics.

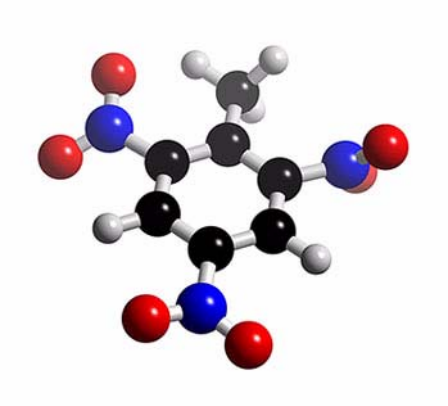

Fig. 1. The molecular structure of 2,4,6 trinitrotoluene (TNT). The carbon, hydrogen, oxygen and nitrogen atoms are coloured black, white, red and blue respectively. (For interpretation of colour mentioned in this figure the reader is referred to the on-line version of the article.)

2. Experimental methods

TNT is known to exist in at least four different forms, two of which are monoclinic and two orthorhombic [6−12]. The common monoclinic [6,7] and orthorhombic [8] forms both have a crystallographic repeat unit which consists of two molecules, so both groups of ν_+ and ν_- ^{14}N NQR transitions consist of six lines. The monoclinic TNT is the stable polymorph up to its melting point at 81°C although the metastable orthorhombic form can survive for long periods at ambient temperatures, but it converts to monoclinic near 70°C with a low enthalpy of transformation [7] and can convert slowly at intermediate temperatures. As an explosive TNT is stable to beyond its melting point. For the work here, we used a sample of monoclinic “creamed” TNT phase prepared by melting flakes of TNT which were then seeded with the finely-ground monoclinic form. The orthorhombic phase sample was prepared by fast quenching of the molten form on a cold surface at −10 °C. The two TNT samples were prepared, characterised and supplied to us by the Defence Science and Technology Laboratory, Fort Halstead, U.K.

The ^{14}N NQR measurements presented here were conducted on a Tecmag “Libra” pulsed RF spectrometer. For the line frequency and relaxation time variable temperature work the NQR probe, which had a Q of around 90, consisted of an RF solenoid coil mounted in a screening can inserted into a glass

Dewar filled with silicone oil. A length of coaxial cable connected the coil to parallel tuning and series matching capacitors mounted in a die-cast aluminium box at the mouth of the Dewar. A platinum resistance temperature sensor clamped to the side of the coil screening can was used to monitor and control the temperature via a Eurotherm temperature controller. For low temperature measurements this controlled the solenoid valve of a refrigerated cold finger immersed in the silicone oil bath; the temperature control was to within ±0.5 °C. For high temperature measurements, an immersion heater was used as well as the cold finger so temperature control was better and was within about ±0.25 °C. The immersion heater was constructed from a small 240 V 350 W cartridge heater (RS 837-666) soldered concentrically to the end of a length of stainless steel tube through which the connecting wires passed to the temperature controller. A capillary thermostat (RS 561-460) mounted on the stainless steel tube above the heater was wired in series with the heater to provide an over-temperature safety cut out should the temperature controller fail in such a way that the heater was full on, an important precaution when studying explosive materials. A length of copper sheet was fitted to the cartridge heater to provide better conduction through the oil bath. The temperature range selected (−30°C to +50°C) was regarded as appropriate for conditions likely to be encountered in mine clearance and other security operations. T_1 relaxation times were mostly measured using a steady state method which involved detecting the line concerned with different repeat times between RF pulses (or sequences of pulses) covering the range up to 5 or 6 times T_1. Plots of peak spectral line intensity versus repeat time gave T_1 recovery curves from which T_1 values were obtained from fits assuming single component exponential T_1 relaxation. To speed up signal collection at the lowest temperatures, pulsed spin-locking (PSL) [2 − 5] echo summation sequences were used to enhance the TNT signals. Shorter T_1 values at high temperature, were measured using the inversion recovery method and for some temperatures and NQR lines the T_1 measurements were repeated with both methods and the results were found to be in reasonable agreement. Good fits to the T_1 recovery curves were obtained with a single exponential term. T_{2e} was measured using a PSL sequence, each sequential data block of a full PSL sequential echo signal train was Fourier transformed and the peak real spectral line intensity of each block used to plot decay curves from which T_{2e} was obtained using the exponential fit $A_0 e^{-2\tau/T_{2e}}$.

.

3. Results and discussion

3.1. Temperature variation of TNT ^{14}N NQR frequencies

The ^{14}N NQR ν_+ and ν_- line frequencies as a function of temperature have already been published for both the monoclinic and orthorhombic form of TNT [1,2,3,13,14]. Over the temperature range −30°C to +50°C (243 K to 323 K) used for our measurements here the variation of line frequency with temperature is close to linear. There is no evidence for any large-amplitude whole-molecule

motion nor interconversion between the two non-equivalent molecules in each form of TNT. A major contribution to this temperature dependence is expected to come from those librational modes involving torsional oscillation of the NO_2 group, which at constant volume should follow the Bayer-Kushida equation [15]

$$\nu(T) = \nu(0) - (3\hbar\nu_0 / 2)\sum_i \frac{A_i}{\omega_i}\left(\frac{1}{\exp(\hbar\omega_i / kT) - 1}\right) \quad (1)$$

where the zero temperature term $\nu(0)$ is given by:-

$$\nu(0) = \nu_0\left[1 - (3/4)\hbar\sum_i A_i / \omega_i\right]$$

ω_i is the librational oscillation frequency of the ith mode, $\nu(T)$ is the NQR line frequency at a temperature T, and ν_0 the resonance frequency in a fictitious "static" lattice. A_i consists of two terms. The first is due to the averaging of the electric field gradient at the nuclear site by the torsional oscillations of the NO_2 group, for which $A_i = 1/I_i$ (I_i being the corresponding moment of inertia), and the second is due to molecular distortion. The temperature variation of the NQR line frequencies in the 243 to 323 K linear region can be described by Eq. (2), a linear form of Eq. (1) obtained by taking the first 2 elements of the Taylor series for the exponential term and assuming one torsional mode ω_t, viz. that about the C– NO_2 bond, to be the main contributor.

$$\nu(T) = \nu(0) - \frac{3\nu_0}{2I_t(\omega_t)^2}.kT = \nu(0) - bT \quad (2)$$

The values of $\nu(0)$ and the temperature coefficient b for all the ν_+ and ν_- lines of both polymorphic forms obtained from linear fits to our line frequency measurements in the 243 – 323 K temperature range are given in Table 1. Table 1 also shows the twist angle of the plane of the nitro groups with respect to that of the benzene ring and the site assignments [14] to the two ortho (oA and oB) and para (p) nitro groups of the two molecules (I and II) of the crystallographic repeat unit. In both polymorphs, the lowest value of b and the twist angle are found for the two para nitro groups which from Eq. (2) should therefore have the higher torsional frequencies. We assume I_t to be 64.6 x 10^{-47} kg m^2 for a nitro group [16] and approximate ν_0 as 875 kHz which is the mean value of the 6 ν_+ frequencies at 77 K [1] where the temperature variation is levelling off. The mean torsional frequency of the para groups is then calculated to be 91 cm^{-1} and that for the ortho groups should cover a range from approximately 60 to 90 cm^{-1}. Similar values have been observed in other aromatic nitro compounds [17-21]. Also the terahertz spectrum of TNT [22,23] shows a number of features, broad peaks or inflections, from 60 to 100 cm^{-1}. A theoretical analysis [24] suggests that these features are “cog-wheel” torsional modes involving the 2,6 NO_2 groups with

the adjacent methyl group and predicts frequencies close to 70 and 91 cm^{-1} for the two molecules (I and II) of the crystallographic repeat unit.

Table 1

^{14}N NQR ν_+ and ν_- line frequencies for monoclinic and orthorhombic TNT have previously been published over a range of temperatures [1,2,3,13,14].This table presents the linear fit parameters, $\nu(0)$ and temperature coefficients *b*, of Eq. 2 for the ν_+ and ν_- NQR lines of both polymorphs of TNT, obtained from our line frequency measurements in the 243 – 323 K temperature range. As elsewhere in this paper NQR lines are identified by their frequency at 22 °C (295 K). The NO_2 site assignments for each line are shown along with the twist angle of the plane of the NO_2 groups obtained from the crystallographic data [6]. The labels I and II distinguish each molecule of the pairs in a unit cell, A and B label different ortho nitro groups.

	Monoclinic TNT				Orthorhombic TNT			
Site	ν_+ [kHz]	$\nu_+(0)$ [kHz]	*b* [Hz K^{-1}]	Twist ∠ [°]	ν_+ [kHz]	$\nu_+(0)$ [kHz]	*b* [Hz K^{-1}]	Twist ∠ [°]
oA-I	859.2	921.18	210.2	60	841.7	891.61	169.2	60
oA-II	842.8	892.50	168.5	50	860.9	924.41	215.0	51
oB-I	848.3	893.50	152.9	41	848.1	891.02	145.4	41
oB-II	837.1	870.29	112.5	46	837.1	872.05	118.4	46
p-I	844.2	875.73	107.0	33	846.5	874.88	96.3	33
p-II	870.3	900.66	103.0	22	868.3	894.98	90.4	22
Site	ν_- [kHz]	$\nu_-(0)$ [kHz]	*b* [Hz K^{-1}]	Twist ∠ [°]	ν_- [kHz]	$\nu_-(0)$ [kHz]	*b* [Hz K^{-1}]	Twist ∠ [°]
oA-I	751.1	819.98	233.4	60	752.1	819.62	228.6	60
oA-II	768.7	821.48	178.7	50	768.9	823.13	183.6	51
oB-I	739.6	786.50	159.0	41	741.3	782.40	139.1	41
oB-II	742.9	782.81	135.2	46	741.3	782.40	139.1	46
p-I	713.9	741.14	92.4	33	712.5	735.91	79.2	33
p-II	714.4	740.36	87.9	22	716.6	742.59	88.0	22

Marino et al. [1,2] measured the ^{14}N NQR ν_+ and ν_- line frequencies for monoclinic TNT from 77 K to 321 K and for orthorhombic TNT from 77 K to 280 K. The line frequency variation with temperature is non-linear over these wide ranges with the rate of change decreasing to low temperature so reported temperature coefficients will vary somewhat depending on the temperature range selected for a linear fit. We compared the reported line frequencies [2] of both forms of TNT in the 243 to 323K temperature range by including them in plots of our data with the linear fits from this work and found good agreement between the two sets of measurements. The temperature coefficients of each NQR line of monoclinic TNT calculated from the data of Marino et al. are also tabulated in reference [3] and these values are shown in Table 2 along with our *b* values from Table 1 for comparison. There is good overall agreement between the two sets of values of *b* for monoclinic TNT with a mean difference of about 6% and largest difference of 12%, for the 844 kHz line. Table 2 also compares our *b* values for orthorhombic TNT with previously published values [36] and the overall agreement is good with a mean difference of about 8%, however here the largest difference is higher at 22%, for the 837 kHz line.

Table 2
The temperature coefficients b (Eq. 2) and the T_1 values measured here compared to previously reported values for the ν_+ and ν_- NQR lines of both polymorphs of TNT. For monoclinic TNT the T_1 values are for 22 °C from the work here and room temperature from Ref. [3]. For orthorhombic TNT the T_1 values are for 20 °C from the work here and 23 °C from Ref. [36].

Monoclinic TNT					Orthorhombic TNT				
Line	b [Hz K^{-1}]		T_1 [s]		Line	b [Hz K^{-1}]		T_1 [s]	
[kHz]	Here	Ref.[3]	Here	Ref.[3]	[kHz]	Here	Ref.[36]	Here	Ref.[36]
870.3	103.0	109	3.0	4.0	868.3	90.4	98	8.0	5.0
859.2	210.2	223	12.0	3.0	860.9	215.0	177	15.0	7.5
848.3	152.9	151	13.0	9.6	848.1	145.4	134	17.0	5.5
844.2	107.0	121	6.5	4.7	846.5	96.3	104	10.0	15.0
842.8	168.5	181	4.5	3.5	841.7	169.2	195	8.0	9.0
837.1	112.5	122	4.3	2.1	837.1	118.4	152	6.0	5.5
768.7	178.7	190	16.0	9.8	768.9	183.6	183	12.0	8.5
751.1	233.4	241	3.0	2.2	752.1	228.6	220	3.5	6.0
742.9	135.2	148	4.0	3.0	741.3	139.1	152	11.0	8.0
739.6	159.0	169	9.0	5.5	741.3	139.1	152	11.0	8.0
714.4	87.9	94	4.0	4.3	716.6	88.0	85	12.5	10.0
713.9	92.4	94	10.0	4.3	712.5	79.2	79	6.0	10.5

For TNT detection applications, since sensitivity increases with frequency, the obvious choice is to work with the ν_+ NQR lines and usually the highest frequency lines at 870 kHz for monoclinic TNT and 868 kHz for orthorhombic TNT. Importantly these lines, which are both associated with the para-nitro groups, also have the lowest temperature coefficients making them the best choice for detecting this explosive when the temperature of the sample is uncertain. When the sample temperature is known and multiple resolved lines are detected, it is possible to use a “finger print” of line frequencies (usually the four lines from 848 to 837 kHz), to enhance the signal-to-noise ratio (SNR) using approximate maximum likelihood parametric data processing [25].

3.2. The ^{14}N NQR relaxation times and signal decay times of TNT

We have measured the ^{14}N NQR spin-lattice relaxation time T_1 for all 12 ν_+ and ν_- lines of both TNT polymorphs at various temperatures in the range 243 – 323 K and we have measured the temperature dependence of T_1 for some lines. The T_1 values obtained here for monoclinic TNT at 22°C (295 K) and orthorhombic TNT at 20°C (293 K) are presented in Table 2 where they are compared to the previously published values for orthorhombic TNT [36] at 23°C and monoclinic TNT [3] presumably at room temperature. Our T_1 values for nineteen of the NQR lines in Table 2 are in reasonable agreement with the previously reported values but four of our T_1 values are significantly different. For monoclinic TNT our T_1 values for the 859 kHz and 713.9 kHz lines are 12 s and 10 s respectively compared to the previously reported [3] values of 3 s and 4.3 s. For orthorhombic TNT our T_1 values for the 861 kHz and 848 kHz lines are 15 s and 17 s respectively compared to the published [36] values of 7.5 s and 5.5 s.

Fig. 2 presents results from our study of the temperature dependence of T_1 for a few of the ν_+ lines of monoclinic and orthorhombic TNT selected to show both the variation of T_1 and in the spread of T_1 values with temperature. In detection applications the variation of T_1 with temperature can have significant impact on detection sensitivity or detection time.

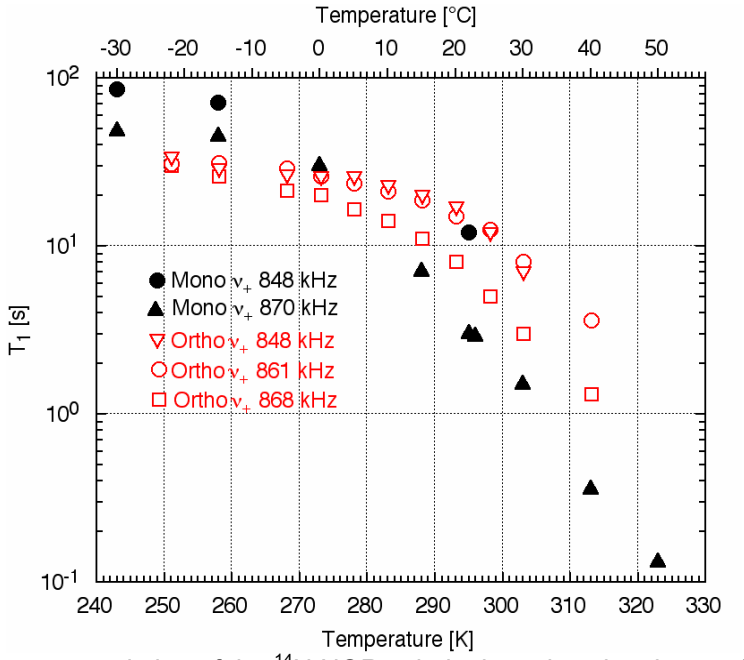

Fig. 2. The temperature variation of the ^{14}N NQR spin-lattice relaxation time T_1 for a few of the ν_+ lines of monoclinic and orthorhombic TNT.

NQR spin-lattice relaxation times T_1 can be strongly influenced by slow molecular rotations and T_1 often becomes shorter to higher temperatures as such processes become more important, the temperature dependence of T_1 can then be used to gain some insight into such molecular dynamics [34,35,15]. Fig. 3 is an Arrhenius plot of our measurements of the temperature variation of the ^{14}N NQR T_1 for the highest frequency ν_+ 870 kHz and ν_- 769 kHz lines of monoclinic TNT and the highest frequency ν_+ 868 kHz line of orthorhombic TNT. The temperature variation falls into two regions with a step in the range 280 – 290 K and Fig. 3 shows linear fits for each region using Eq. (3); the logarithmic form of the Arrhenius equation.

$$\ln(T_1) = \ln(A) + \frac{E_a}{R}\left(\frac{1}{T}\right) \qquad (3)$$

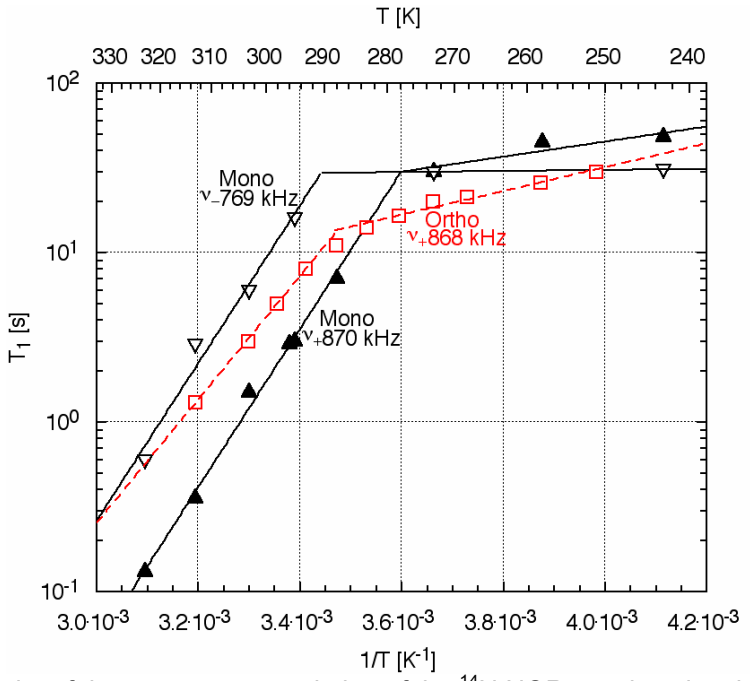

Fig. 3. Arrhenius plot of the temperature variation of the ^{14}N NQR T_1 relaxation time for the ν_+ 870 kHz and ν_- 769 kHz lines of monoclinic TNT and the ν_+ 868 kHz line of orthorhombic TNT. The line plots are linear fits using Eq. (3).

From the fits to the region of interest here, the higher temperature region above 280 – 290 K, we obtain an activation energy E_a of 89 kJ mol^{-1} for both the lines of monoclinic TNT while for the orthorhombic line we obtain the lower value of 70 kJ mol^{-1} for E_a. In the lower temperature region the activation energies are 8.5, 0.6 and 13 kJ mol^{-1} for the ν_+ 870 kHz, ν_- 769 kHz lines of monoclinic TNT and the ν_+ 868 kHz line of orthorhombic TNT respectively.

The trains of echoes generated by multiple pulse sequences of the pulse spin-locking (PSL) type [2 − 5] decay with an effective relaxation time $T_{2e} > T_2$ which generally increases as the RF pulse spacing decreases. The echo trains are a mixture of Hahn (or direct) and stimulated echoes, with the latter introducing some T_1 dependence into the echo train decay time. T_{2e} is not a fundamental relaxation time but depends on T_1, T_2, $T_{1\rho}$ (T_1 in the rotating frame) and T_2^*, so the dynamics of the T_{2e} decay will be linked to that of these other relaxation times. Fig. 4 is an Arrhenius plot of our measurements of the temperature variation of T_{2e} for the ν_+ 870 kHz line of monoclinic TNT and the ν_+ 868 kHz line of orthorhombic TNT. T_{2e} was obtained from single exponential fits to echo trains obtained using PSL sequences, as described in section 2, with 2τ pulse spacings of 1.134 ms and 2.2 ms respectively for the monoclinic and orthorhombic TNT. Using the logarithmic form of the Arrhenius equation Eq. (3) for a linear fit to the three monoclinic data points as shown in Fig. 4 we obtain an E_a of 71 kJ mol^{-1} and similarly the linear fit to the eight highest temperature orthorhombic data points yields an E_a of 78 kHz. We have not measured the spin-spin relaxation time T_2 over a range of temperatures but the values we have obtained at two temperatures for the ν_+ 870 kHz line of monoclinic and the ν_+ 868 kHz line of

orthorhombic TNT are also shown in Fig. 4 to illustrate the difference between T_{2e} and T_2 and T_1 (Fig. 4). The two point linear fits for T_2 in Fig. 4 give an estimate of E_a of 44 kJ mol^{-1} for the 870 kHz line of monoclinic TNT and 31 kJ mol^{-1} for the 868 kHz line of orthorhombic TNT.

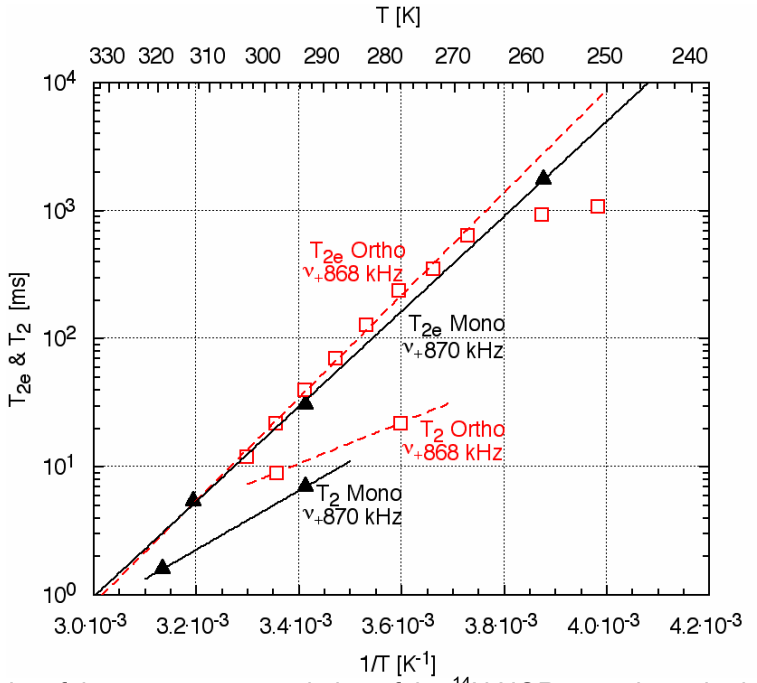

Fig. 4. Arrhenius plot of the temperature variation of the ^{14}N NQR T_{2e} echo train decay time and T_2 relaxation time for the ν_+ 870 kHz line of monoclinic TNT and the ν_+ 868 kHz line of orthorhombic TNT. The line plots are linear fits using Eq. (3).

The high temperature activation energies are summarised in Table 3. The most likely explanation for the high temperature variation of T_1 and T_{2e} is that they are both governed by the effects of hindered rotation of the NO_2 group about the C–NO_2 bond. This model may be supported by ^{17}O double resonance NMR/NQR experiments which show that no ^{17}O signals from the NO_2 groups could be detected above 230 K [26]. This may be due to a broadening of the lines caused by interchange of the oxygen atoms following rotation of the NO_2 group, which would produce a considerable change in the electric field tensor at the oxygen site. We have found from similar work on the temperature variation of T_1 in the explosive RDX [27] that E_a is 92 kJ mol^{-1} for hindered rotation about the N–NO_2 bond and for the explosive PETN [16] that E_a is 24.5 kJ mol^{-1} for rotation about the O–NO_2 bond. In the isolated TNT molecule the energy barrier for nitro group rotation is calculated to be 10.6 kJ mol^{-1} [24], indicating that solid state interactions must make a major contribution to our measured values. For C–NO_2 groups in other molecules, where this behaviour is expected to be a common feature [28,29], the literature values for otational activation energies vary considerably. For example they are estimated to be larger than 31 kJ mol^{-1} in m-chloronitrobenzene [17], 22.7 kJ mol^{-1} for the para and 35.4 kJ mol^{-1} for the ortho NO_2 groups in 2,4-dinitrochlorobenzene [18], close to 12 kJ mol^{-1} in 3− and 4−nitrobenzene sulphonyl chlorides but 29 kJ mol^{-1} for the 2−form [19], 27.4 and

31.2 kJ mol^{-1} for the two ortho groups in 2,4,6-trinitrochlorobenzene (picryl chloride) [20] and 17.5 kJ mol^{-1} in 1-chloro-2,4-dinitrobenzene but a mean value of 13.6 kJ mol^{-1} in 1,2-dichloro-3-nitrobenzene [21]. In gaseous nitrobenzene, a planar molecule, values of 12 ± 6 [30] and 17 ± 4 kJ mol^{-1} [31] have been measured. These values seem to bear little relationship to the C–N bond length; its average values in the two molecules in the monoclinic form of TNT are 147.5 pm [6] and 148.2 pm [8], in the orthorhombic form the average of the two is 147 pm and in gaseous nitrobenzene 146.8 pm [31]. Our values of $E_a(T_1)$ in Table 3 suggest there is little difference between the ortho and para NO_2 groups in monoclinic TNT since for both the activation energies are close to 90 kJ mol^{-1} but for orthorhombic TNT, at least for the para group, $E_a(T_1)$ is somewhat lower at 70 kJ mol^{-1}. However, comparisons between these E_a values may not be very meaningful in view of the likely variations in the shape of the potential energy curves. In the case of TNT, one reason for the variations listed in Table 1; the para NO_2 groups may need to rotate by only 44° to reach an almost equivalent energy position, whereas this angle would need to lie between 92° and 120° for the ortho NO_2 groups.

Table 3

The high temperature activation energies E_a for T_1, T_{2e} and T_2 of the ν_+ 870 kHz and ν_- 769 kHz lines of monoclinic TNT and the ν_+ 868 kHz line of orthorhombic TNT obtained from the fits using Eq. (3) in Figs. 3 & 4 as discussed in the text.

Site	Monoclinic TNT				Orthorhombic TNT			
	Line [kHz]	E_a [kJ mol^{-1}]			Line [kHz]	E_a [kJ mol^{-1}]		
		E_a (T_1)	E_a (T_{2e})	E_a (T_2)		E_a (T_1)	E_a (T_{2e})	E_a (T_2)
p-II	ν_+ 870	89	71	44	ν_+ 868	70	78	31
oA-II	ν_- 769	89	—	—	—	—	—	—

We have examined the ν_+ 870 kHz spectral line of monoclinic TNT at various temperatures and found the line shape to be a good fit to a Lorentzian profile for which the full width at half height $\Delta\nu_{1/2}$ is related to the signal decay time T_2^* via $\Delta\nu_{1/2} = 1/(\pi T_2^*)$. Lorentzian line shapes are expected when the dominant term is damping of the Larmor precession of the magnetization in the electric field gradient due to relaxation [32]. The temperature variation of $\Delta\nu_{1/2}$ is shown in Fig. 5 together with a plot of the natural width $\Delta\nu_{1/2} = 1/(\pi T_2)$ obtained from the parameters of the fit to T_2 in Fig. 4.

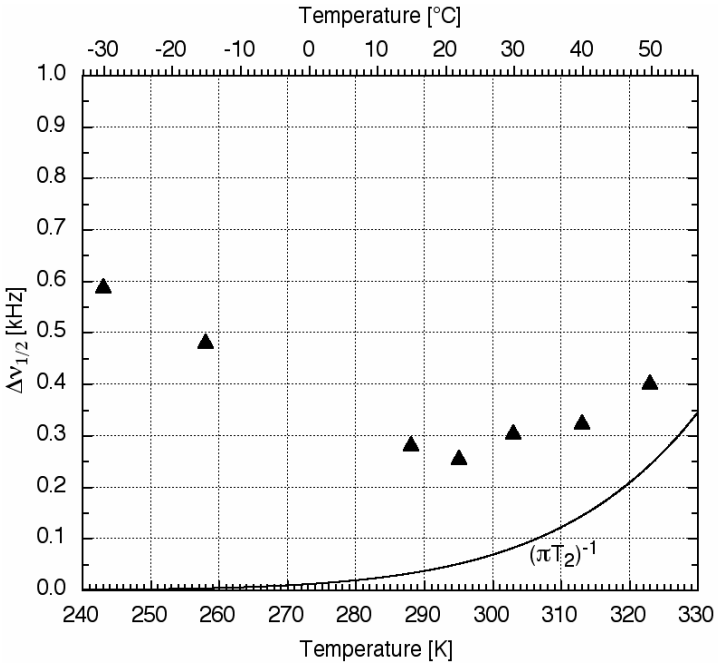

Fig. 5. The temperature variation of full width at half height $\Delta\nu_{1/2}$ for the ν_+ 870 kHz ^{14}N NQR line of monoclinic TNT and a plot of the natural width $\Delta\nu_{1/2} = 1/(\pi T_2)$ obtained from the parameters of the fit to T_2 in Fig. 4.

Recognising that the observed line shape function is a convolution of inhomogeneous broadening and the natural line shape function and assuming both to be Lorentzian we can write [27]:-

$$1/T_2^* = 1/T_{2(\text{Inhom})} + 1/T_2 \qquad (4)$$

where $T_{2(\text{Inhom})}$ is the inhomogeneous decay time. Since T_2 increases to lower temperature $1/T_2$ rapidly becomes negligible and we have $(1/T_{2(\text{Inhom})})_{T=0} = (1/T_2^*)_{T=0}$. Fig. 6 shows the temperature dependence of $1/T_{2(\text{Inhom})}$ calculated via Eq. (4) and the data in Fig.5. From the linear fit, which represents the temperature dependence of $1/T_{2(\text{Inhom})}$ as

$$1/T_{2(\text{Inhom})}(T) = [\,(1/T_{2(\text{Inhom})})_{T=0} + \alpha\, T] \;\text{ or }\; [(1/T_2^*)_{T=0} + \alpha\, T] \qquad (5)$$

we obtain α, the temperature coefficient of $1/T_{2(\text{Inhom})}$, as -0.018 $\text{ms}^{-1}\text{K}^{-1}$. This has the same sign but is a factor of four larger than value of α observed for RDX [27] where it was attributed to changes in the torsional frequency of the NO_2 groups at dislocations. This may also be the case for TNT since the major defects in TNT crystals are growth-induced defects such as growth sectors and boundaries, solvent inclusions, edge or screw dislocations and stacking faults [33]. The parameter α may of course be sample dependent and could provide some information on sample origin.

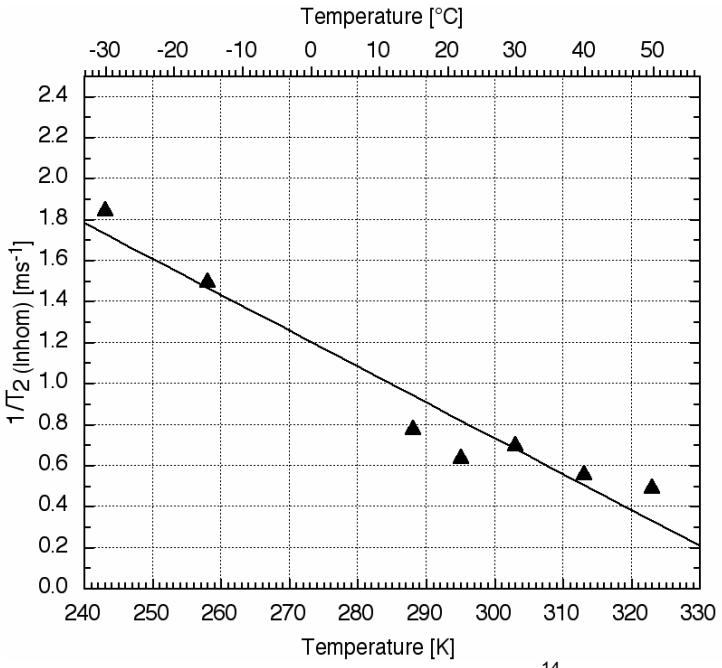

Fig. 6. The temperature variation of $1/T_{2(\mathrm{Inhom})}$ for the ν_+ 870 kHz ^{14}N NQR line of monoclinic TNT. The line plot is a linear fit using Eq. 5.

4. Conclusions

We have measured the various ^{14}N NQR parameters for a number of the ν_+ and ν_- lines of monoclinic and orthorhombic TNT over a range of temperatures and discussed the temperature variation of some of these parameters in terms of the molecular dynamics. The temperature dependence of T_1 has been explained as due to hindered rotation of the NO_2 group about the C–NO_2 bond with an activation energy of 89 kJ mol^{-1} for the ortho and para groups of monoclinic TNT and 70 kJ mol^{-1} for the para group of orthorhombic TNT.

Acknowledgement

We thank the Defence Science and Technology Laboratory (DSTL) at Fort Halstead, UK for support of this project and we are grateful to Dr. Iain Poplett for helpful discussions.

References

[1] R.A. Marino and R. F. Connors, Orthorhombic and Monoclinic TNT: A Nitrogen-14 NQR Study, J. Mol. Struct. 111 (1983) 323 – 328.

[2] R.A. Marino, R. F. Connors and L. Leonard, Nitrogen−14 NQR Study of Energetic Materials, Final Report, Block Engineering (1982).

[3] J.B. Miller, Nuclear Quadrupole Resonance Detection of Explosives, In: J. Yinon (Ed), Counterterrorist Detection Techniques of Explosives, Elsevier, (2007).

[4] R.A. Marino and S.M. Klainer, Multiple Spin Echoes in Pure Quadrupole Resonance, J. Chem. Phys. 67 (1977) 3388 – 3389.

[5] S.S. Kim, J.R.P. Jayakody and R.A. Marino, Experimental Investigations of the Strong Off-Resonant Comb (SORC) Pulse Sequence in ^{14}N NQR, Z. Naturforsch. 47a (1992) 415 – 420.

[6] J.R.C. Duke, Crystallography of TNT, ERDE Report WAA 264/040. (1974).

[7] R.M. Vrcelj, J.N. Sherwood, A.R. Kennedy, H.G. Gallagher and T. Gelbrich, Polymorphism in 2-4-6 Trinitrotoluene, Crystal Growth and Design, 3 (2003) 1027 – 1032.

[8] W.R. Carper, L.P. Davies and M.W. Extine, Molecular Structure of 2,4,6-Trinitrotoluene, J. Phys. Chem. 86 (1982) 459 – 462.

[9] H.G. Gallagher and J.N. Sherwood, The Growth and Perfection of Single Crystals of TNT, Mat. Res. Soc. Symp. Proc. 296 (1993) 215 – 219.

[10] H.G. Gallagher and J.N. Sherwood, Polymorphism, twinning and morphology of crystals of 2,4,6-trinitrotoluene grown from solution, J. Chem. Soc. Farad. Trans. 92 (1996) 2107 – 2116.

[11] D.C. Grabar, F.C. Rauch and A.J. Fanelli, Observation of solid-solid polymorphic transformation in 2,4,6-trinotrotoluene, J. Phys. Chem. 73 (1969) 3514 – 3516.

[12] N.I. Golovina, A.N. Titkov, A.V. Raeviskii and L.O.Atovmyan, Kinetics and mechanism of phase transitions in the crystals of 2,4,6-trinitrotoluene and benzotrifuroxane, J. Sol. State Chem. 113 (1994) 229 – 238.

[13] J.A.S. Smith, M.D. Rowe, R.M. Deas and M.J. Gaskell, Nuclear Quadrupole Resonance Detection of Landmines, The Proceedings of EUDEM2-SCOT-2003, International Conference on Requirements and Technologies for the Detection, Removal and Neutralization of Landmines and UXO, Vol.2 (2003) 715 – 721. VUB, Brussels, Belgium.

[14] R.M. Deas, M.J. Gaskell, K. Long, N.F. Peirson, M.D. Rowe and J.A.S. Smith, An NQR study of the crystalline structure of TNT, Proc. SPIE, 5415 (1) (2004) 510 – 520.

[15] H.Chihara and N.Nakamura, Study of molecular motion by nuclear quadrupole resonance and relaxation, Adv. Nucl. Quad. Reson. Ed. J.A.S.Smith 4 (1980) 1 – 69.

[16] J.A.S. Smith, T.J. Rayner, M.D. Rowe, J. Barras, N.F. Peirson, A.D. Stevens and K. Althoefer, Magnetic field-cycling NMR and ^{14}N, ^{17}O quadrupole resonance in the explosive pentaerythritol tetranitrate (PETN), J. Magn. Reson. 204 (2010) 139 –144.

[17] J. Schneider, C.A. Meriles, L.A.de O. Nunes and S.C. Perez, The dynamics of the NO_2 group in the solid phase of *m*-chloronitrobenzene studied by Raman spectroscopy and ^{35}Cl NQR, J. Mol. Struct. 447 (1998) 13 –19.

[18] C. Mattea and A.H. Brunetti, Nuclear quadrupole resonance in 2,4-dinitrochlorobenzene, J. Mol. Struct. 594 (2000) 215 – 210.

[19] S.C. Perez, M. Krupski, R.L. Armstrong and A.H. Brunetti, An NQR study of the thermally activated motion of the nitro groups in 3-nitrobenzene sulphonyl chloride, J. Phys. Condens. Matter. 6 (1994) 6019 – 6026.

[20] I.A. Kyuntsel, ^{36}Cl NQR study of thermo-activated motions of nitro groups in picryl chloride, Z. Naturforsch. 51a (1996) 713 – 715.

[21] J. Srinivas, R.K. Subramanian, K.P. Ramesh, J. Ramakrishna, K.S. Suresh and C.R. Rao, ^{35}Cl NQR studies of 1-chloro-2,4-dinitrobenzene and 1,2-dichloro -3- nitrobenzene as a function of temperature and pressure, Magn. Reson. Chem. 40 (2002) 337 – 345

[22] M.J. Tribe, D. Schauki, C.A. Kelly and R. Osiander, THz imaging and spectroscopy of landmine detection, in Terahertz and Gigahertz Electronics and Photonics III, ed. R.J.Hwu, Proc. SPIE. 5354 (2004) 168.

[23] M.R. Leahy-Hoppa, M.J. Fitch, X. Zheng, L. M. Hayden and R. Osiander, Wideband terahertz spectroscopy of explosives, Chem. Phys. Lett. 434 (2007) 227 – 230.

[24] J. Clarkson, W.E. Smith, D.N. Batchelder, D.A. Smith and A.M. Coats, A theoretical study of the structure and vibrations of 2,4,6-trinitrotoluene, J. Mol. Struct. 648 (2003) 203 – 214.

[25] A. Jakobsson, M. Mossberg, M.D. Rowe and J.A.S. Smith, Exploiting temperature dependency in the detection of NQR signals, IEEE Trans. Signal Proc. 54 (2006) 1610 – 1616.

[26] J. Seliger, V. Žagar, R. Blinc and F. Milia, Temperature dependence of ^{17}O and ^{14}N NQR frequencies in commercial TNT, Appl. Magn. Reson., 29 (2005) 541 – 548.

[27] J.A.S. Smith, M. Blanz, T.J. Rayner, M.D. Rowe, S. Bedford and K. Althoefer, ^{14}N quadrupole resonance and ^{1}H T_1 dispersion in the explosive RDX, J. Magn. Reson. 213 (2011) 99 – 108.

[28] A.Weiss, The Combination of X-ray diffraction and nuclear quadrupole resonance studies of crystals, Acta Crystall. B51 (1995) 523 – 539.

[29] A. Weiss and S. Wigand, Correlation of NQR and chemical bond parameters, Z. Naturforsch. 45a (1990) 195 – 212.

[30] J.M. Høg, L. Lygaard and G.Ole. Sørenson, Microwave spectrum and planarity of nitrobenzene, J. Molec.Struct. 7 (1971) 111 – 121.

[31] O.V. Dorofeeva, Y.V. Vishnefvsky, N. Vogt, J. Vogt, L.V.Khristenko, S. V.Krasnoshchekov, I.G. Shishkov, I. Hargittai and L.V. Vilkov, Molecular structure and conformation of nitrobenzene reinvestigated by combined analysis of gas-phase electron diffraction, rotational constants and theoretical calculations, Struct. Chem. 18 (2007) 739 – 753.

[32] D.F. Howarth, J.A. Weil and Z. Zimpet, Generalisation of the line-shapes useful in magnetic resonance spectroscopy, J. Magn. Reson. 161 (2003) 215 – 221.

[33] H.G. Gallagher, R.M. Vrcelj and J.N. Sherwood, The crystal growth and perfection of 2,4,6-trinitrotoluene, J. Cryst. Growth 250 (2003) 486 – 498.

[34] S. Alexander and A. Tzalmona, Relaxation by Slow Motional Processes. Effect of Molecular Rotations in Pure Quadrupole Resonance, Phys. Rev. 138 (1965) A845 – A855.

[35] A. Tzalmona, Anisotropy of Molecular Rotations Measured by NQR Relaxation, J. Chem. Phys. 50 (1969) 366 – 372.

[36] V.T. Mikhaltsevitch and T.N. Rudakov, On the NQR detection of nitrogenated substances by multi-pulse sequences, Phys. Stat. Sol. 241 (2004) 411 – 419.